Journal of Environmental Science and Engineering A 6 (2017) 594-605
doi:10.17265/2162-5298/2017.12.002

Improved Model for Semideciduous Seasonal Forest Production of Leaves and Deciduousness

Thomaz Costa

Core of Water, Soil and Environmental Sustainability (NSAM), Embrapa Maize and Sorghum, Sete Lagoas 35701-970, Brazil

Abstract: The climate, mainly the water availability and temperature, drives the renewal of biomass in seasonal forest ecosystem, and the greenness and leaf area of its canopy are responsive by climate variations. This study verified models to explain the phenomenon of leaf production and deciduousness by time, with LAI (Leaf Area Index), NDVI (Normalized Difference Vegetation Index) and climate variables, on period 2011-2016. The data were obtained in satellite images and in plots installed at forest monitoring sites, visited monthly. The analysis incorporated the water balance. Three equations were compared, two already published and the equation that was adjusted in this work. The model was improved and validated with new variables and data. It is possible to estimate the fall and renew of leaves biomass in semideciduous forests with reasonable precision.

Key words: Ecosystem dynamics, climate variables, LAI, NDVI.

1. Introduction

Leaf production and deciduousness are phenomena that occur with a little temporal overlay in semideciduous forests, because it is a typology conditioned by tropical climatic seasonality, with a period of intense summer rains, and another of severe drought, dependent of the dynamics of soil water and change of temperature [1].

The sprouting and leaf growth, the senescence and the leaf fall are crucial for forestry ecosystem maintenance and for survival through the nutrient cycling sustained by deciduousness. The fall of leaves, branches, flowers and fruits supply organic material to the surface layer of the soil, nourishing the plant species. Using this process, nutrients are deposited and mineralized, maintaining the soil fertility in these ecosystems [2-4].

The type of vegetation (floristic diversity) and the environmental conditions (temperature and water stress) influence the distribution, quantity and quality of these materials, which form the litterfall [5-7].

Corresponding author: Thomaz Costa, Ph.D., main research field: remote sensing of vegetation.

The quantity of material that falls from the canopy, forming the litterfall, reaches a rate of tons per hectare/year. The forest starts producing leaves again in rainy season beginning, renewing the lost biomass. Potithep, S., et al. [8] and Kale, M., et al. [9] stablished two stages in deciduous tropical forests, leaf growth and senescence.

In order to understand the year-to-year cycling pattern of the carbon in the terrestrial ecosystems, attempts to detect the vegetation phenological patterns by remote sensing had been made, especially after the release of the MODIS (Moderate Resolution Imaging Spectroradiometer) sensor, with calibration quality and the products provided, such as LAI (Leaf Area Index) and fAPAR (fraction of Absorbed Photosynthetically Active Radiation) [10-12].

One part of this carbon is in deciduousness phenomenon that can be modeled by means of relationships with climatic, biophysics and orbital variables, allowing estimates of leaf fall [13] and annual CO_2 capture estimates [14]. However, this modelling still needs improvement, which is the objective of this work.

2. Material and Methods

2.1 Study Site

The Köppen climatic classification for Sete Lagoas is Cwa [15], which indicates Savana climate with dry winter and rainy summer. The annual average temperature is 21.1 °C. The annual rainfall is 1,384 mm and the annual evapotranspiration is around 1,444 mm [16].

The monitoring was done in three sites (51, 61 and 81) of the semideciduous seasonal forest at biome Savanna, at the Experimental Farm of Embrapa Mize and Sorghum, which is located in the city of Sete Lagoas, State of Minas Gerais, Brazil (Fig. 1), characterized by the parameters of Table 1.

Sites 51 and 61 are in remnants of the semideciduous seasonal forest. The site 51 is on Ultisols Dystrophic Typic and the sites 61 and 81 are on Inceptisols Humic Dystrophic Typic class [17]. The difference among them is that site 81 is close to water bodies.

2.2 Variables and Procedures

The Thornthwaite water balance was calculated from 2011 until October 2016 with daily data of PET (Potential Evapo Transpiration). This procedure is explained in Costa, T. C. C., et al. [14]. The maximum and minimum temperature, relative humidity and wind speed were average on deciduousness periods. The daily values of evapotranspiration, rain, hydric deficit and hydric surplus were accumulated on deciduousness periods.

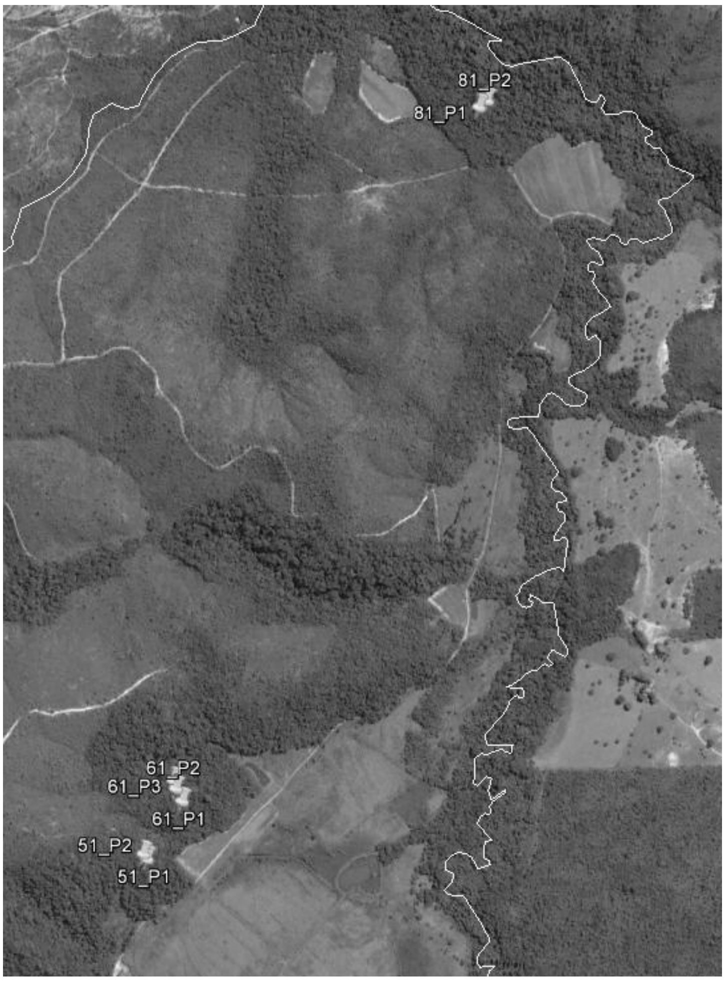

Fig. 1 Location of the sites 51, 61 and 81 in fragment of the north side of the Embrapa Farm, Sete Lagoas, Minas Gerais, Brazil.

Table 1 Coordinates (X, Y) UTM/23 Zone WGS84 of plots with 20 × 20 meters; five nets in each plot; geometric altitude (Z);

declination in degrees (Decl); individual density (ind·m^{-2}); basal area (B); average tree height (H); Shannon index (H'); Simpson dominance index (C) and period of collects.

Site	Plot	X (m)	Y (m)	Z (m)	Decl (°)	D (arv./m^2)	B (m^2/ha)	Tree height (m)	H'	C	Collec. Dlw
51	1	588,363	7,851,128	713	10.2	0.08	15	10.4	2.73	0.05	2011/12
	2	588,352	7,851,142	724	7.2	0.10	36	11.8	2.55	0.08	2011/12
61	1	588,458	7,851,281	736	14.1	0.08	16	8.7	2.19	0.11	2011/12
	2	588,441	7,851,313	735	11.2	0.10	26	12.0	2.20	0.15	2011/12
	3	588,434	7,851,334	729	7.0	0.08	18	11.7	3.03	0.02	2011/12, 2015/16
81	1	589,268	7,853,121	707	6.2	0.19	33	9.0	2.88	0.07	2011/12, 2014/15
	2	589,289	7,853,140	707	7.0	0.17	30	9.4	2.85	0.07	2011/12

In order to measure the deciduousness data, it was used permanent plots of the inventory, to gather of the deposition of litterfall in the nets. The collections were carried out monthly in the approximate period of 30 days. The dry leaves variable (g·m^{-2}) is the average of the five nets in each plot. The leaf area (m^2 of leaf × m^{-2} of soil) was measured with the LAI 2200 Plant Canopy Analyzer [18]. The procedures were described by Costa, T. C. C., et al. [14].

It was selected three Landsat TM 5 images, as they coincide with their final reception, complementing the period with seven images of the IRS LISS3 (Indian Remote Sensing Satellite), a sensor with characteristics closer to Landsat. The main differences between them are the spatial (30 m and 24 m pixel) and radiometric (8 and 7 bits) resolutions, and a small difference in the range of the spectral bands. In 2013, it was used Landsat 8 OLI images with radiometric resolution of 16 bits, and shorter amplitude band compared with Landsat TM 5, mainly in near infrared band.

The geometrical correction was performed in Geotiff Examiner software, with the aid of the graphic software Inkscape, using a reference point to dislocate the images. This form of correction was more precise compared to the polynomial corrections, even with RMS smaller than ½ pixel. In order to extract NDVI (Normalized Difference Vegetation Index) in each permanent plot, it was digitalized a rectangle of nine pixels centralized in the central point of the permanent plot. For Landsat 8 OLI images, geometric corrections were not necessary.

The atmospheric correction was performed with an ATMOSC (Atmospherically Correcting model) module of Idrisi Taiga@, using the full model [19]. The Dn Raze (portion of the spectral response caused by the interference of the atmosphere by scattering and absorption of the radiation in digital number format) [19] was obtained through the smaller spectral response of the visible and near infrared bands, in points of the lakes on region, compared with Gürtler, P. S. J.'s [20] procedure. It was based on the atmosphere correction method of Chavez, S., et al. [21]. All images have visibility above 10 km (information from air traffic control service bulletin of Confins Airport, State of Minas Gerais, Brazil).

The atmosphere optical dimension is the sum of the main components Rayleigh scattering, aerosols scattering and absorption, water vapor and typical ozone absorption. The Rayleigh scattering was adjusted to local height with atmospheric pressure data. The water vapor component was obtained for the NIR (Near Infrared), in function of the relative humidity [19] using the linear relation [14].

The quantity of diffuse energy in relation to the total energy was estimated by SPECTRAL2 model, described in Bird, R. E. and Riordan, C. [22], with the following input parameters: AOD (Aerosol Optical Depth) = exp(-altitude (km)/1.2) × 0.2; albedo; turbity coefficient; column ozone, in centimeters; PWV (Precipitable Water Vapor), in cm, calculated with Abdullrahman Maghrabi and Dajani formulas [23]; pressure of air (mha); and usual variables (satellite time in hour, decimal minute), degree and azimuth of surface.

2.3 Monitoring Period

It was analyzed three variables: dry leaf weight ($g \cdot m^{-2} \cdot period^{-1}$), LAI ($m^2 \cdot m^{-2}$) and NDVI, from 2011 to 2016 (Table 2). The measures were made on approximate days of the month.

In order to obtain data on the same days of the dry leaves collected, NDVI and LAI data were interpolated using the dates. It did not measure the absence of some data in the periods because of project closure (end of support in data collection). Besides, an unforeseen malfunction of the Lai 2200 happened, which resulted in the lack of data between April and July 2016. Regarding the few NDVI data, the justification is the use of only high quality images.

2.4 Improvement of Dry Leaf Weight Modeling

It was compared results of three equations, published in Costa, T. C. C., et al. [13, 14], and those developed in this work.

Table 2 Data of dry leaves weight, LAI and NDVI, of the Landsat 5 TM (08/20/11-09/21/11), IRS (02/08/12-10/05/12), e Landsat 8 OLI (08/09/13-09/13/16) images, with respective days of the year.

Per.	Leaves (g/m^2)		LAI (m^2/m^2)		NDVI		Per.	Leaves (g/m^2)		LAI (m^2/m^2)		NDVI	
	Date	Day	Date	Day	Date	Day		Date	Day	Date	Day	Date	Day
1	07/15/11	196					3	08/27/14	239	08/14/14	226	08/12/14	224
	08/15/11	227			08/20/11	232		09/26/14	269	09/16/14	259	08/28/14	240
	09/13/11	256	09/13/11	256	09/05/11	248		10/28/14	301	10/20/14	293	09/13/14	256
	10/18/11	291	10/19/11	292	09/21/11	264		11/26/14	330	11/19/14	323	10/15/14	288
	11/16/11	320	11/16/11	320				12/23/14	357	12/15/14	349	12/18/14	352
	12/14/11	348	12/12/11	346				01/29/15	394	01/23/15	388		
	01/16/12	381	01/15/12	380				02/27/15	423	02/27/15	423		
	02/14/12	410	02/10/12	406	02/08/12	404		03/27/15	451	03/27/15	451		
	03/15/12	440	03/13/12	438	03/03/12	428		04/29/15	484	04/30/15	485		
	04/15/12	471	04/17/12	473	04/20/12	476		05/27/15	512	05/29/15	514	05/27/15	512
	05/14/12	500	05/08/12	494				06/28/15	544	06/26/15	542		
	06/15/12	532	06/20/12	537	07/01/12	548		07/28/15	574	07/17/15	563	07/30/15	576
	07/15/12	562	07/13/12	560	07/25/12	572	4	08/28/15	240	08/21/15	233	08/15/15	226
	08/14/12	592	08/14/12	592				09/30/15	273	09/25/15	268	09/16/15	258
	09/13/12	622	09/13/12	622	09/11/12	620		10/30/15	303	10/29/15	302	10/02/15	274
			10/17/12	656	10/05/12	644		11/30/15	334	11/25/15	329		
2			08/15/13	227	08/09/13	221		12/29/15	363	12/18/15	352		
			09/16/13	259	09/26/13	269		01/29/16	394	01/25/16	390		
			10/15/13	288	10/28/13	301		02/26/16	422	02/27/16	423		
			11/18/13	322	11/13/13	317		03/28/16	453	04/01/16	457		
			12/17/13	351				04/28/16	484				
			01/27/14	392	01/16/14	381		05/30/16	516				
			02/17/14	413				06/30/16	547				
			03/17/14	441				07/29/16	576				
			04/22/14	477	04/22/14	477				08/19/16	597	08/17/16	594
			05/20/14	505	06/09/14	525							
			06/18/14	534	06/25/14	541							
			07/21/14	567	07/11/14	557							

Journal of Environmental Science and Engineering A 6 (2017) 594-605
doi:10.17265/2162-5298/2017.12.002

3. Results and Discussion

The region where this experiment was carried out has tropical climatic seasonality. Its rainy season ranges from October to March, and the dry season, from April to September. Fig. 2 presents the water balance for the period of study. The difference between surplus and deficit of the water was not made because in this case the short sequence of days without rain is not visible in data analysis. This condition is important in analysis because hydric deficit has relation with deciduousness in summer period.

In Table 3, it can see the correlations of LAI with climate variables. LAI correlates with NDVI (Fig. 3), relative humidity, rain, evapotranspiration, deficiency

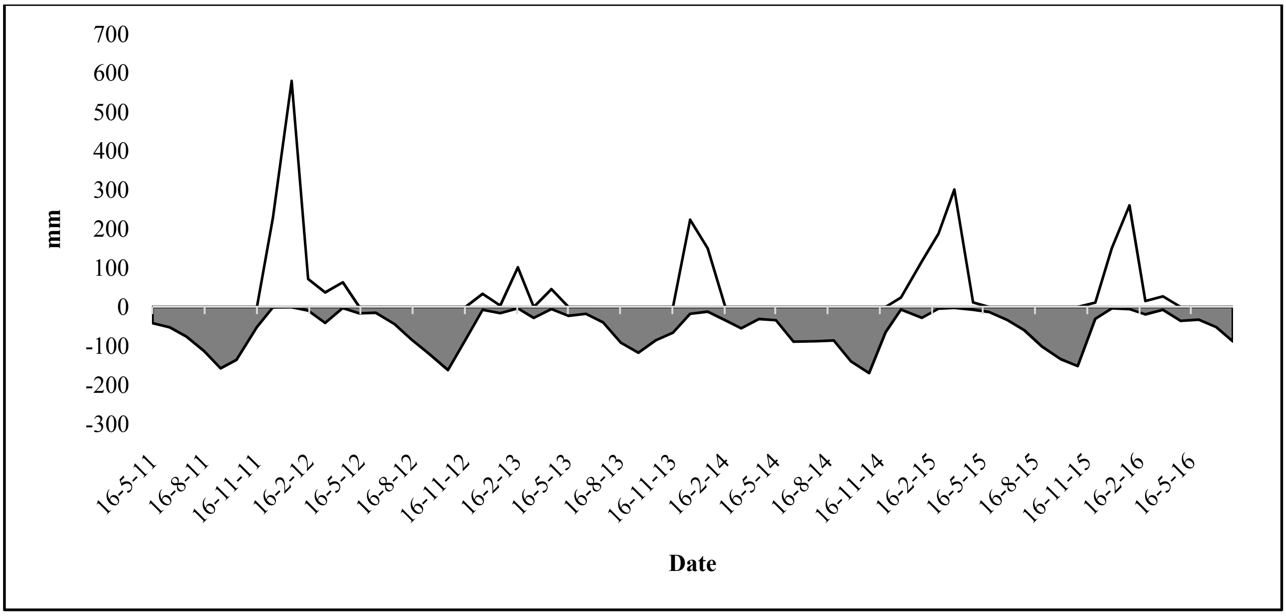

Fig. 2 Accumulated daily climatic water balance of Thornthwaite. Note: DEF (Deficiency) and EXC (Surplus) water to CAD = 150 mm, establishing the same accumulation period of the fallen leaves.

Table 3 Pearson correlations between LAI ($m^2 \cdot m^{-2}$); Dlw (Dry leaf weight ($g \cdot m^{-2} \cdot period^{-1}$)); NDVI (v - ifp)/(v + ifp); Maximum Temperature °C (TMax); Minimum Temperature °C (TMin); Relative Humidity % on 12h (RH12) and on 18h (RH18); Ppt (Rain); ETR (Reference Evapotranspiration); DEF (Water Deficiency (mm)); EXC (Water Excess (mm)); speed wind on 12h (SpWin12) and on 18h (SpWin18). (ns: non-significant at 0.05 of probability, n = 84).

Variables	LAI	Dlw	NDVI	TMax	TMin	RH12	RH18	Ppt	ETR	DEF(-)	EXC	SpWin12
Dlw	-0.53											
NDVI	0.52	-0.28										
TMax	ns 0.01	ns 0.00	0.47									
TMin	0.54	-0.70	0.54	0.34								
UR12	0.53	-0.58	ns 0.05	-0.62	0.35							
UR18	0.55	-0.70	ns 0.17	-0.43	0.65	0.90						
Ppt	0.41	-0.47	ns 0.17	ns -0.19	0.66	0.65	0.78					
ETR	-0.54	0.57	ns -0.01	0.64	-0.23	-0.93	-0.82	-0.50				
DEF(-)	0.70	-0.71	ns 0.20	-0.42	0.43	0.89	0.82	0.49	-0.93			
EXC	0.34	-0.35	ns 0.11	-0.24	0.52	0.63	0.70	0.97	-0.49	0.43		
SpWin12	-0.47	0.49	ns -0.05	0.58	ns -0.10	-0.86	-0.67	-0.42	0.88	-0.83	-0.42	
SpWin18	-0.37	0.55	ns -0.16	0.38	-0.28	-0.62	-0.66	-0.23	0.69	-0.64	ns -0.17	0.71

(-): negative values.

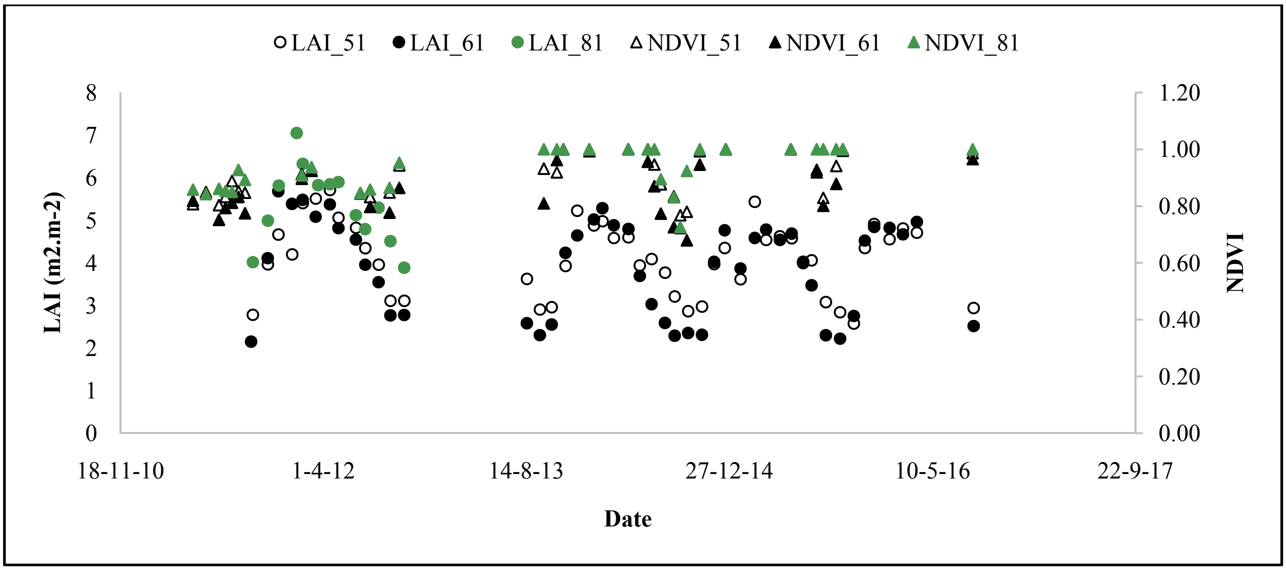

Fig. 3 Relations between NDVI and LAI in sites 51, 61 and 81.

and surplus hydric. LAI also correlates with wind speed and dry leaves, but with opposite signal, in consistent way as well.

LAI had bigger correlation with dry leaf than NDVI (Figs. 4 and 5). The values of NDVI do not have great precision yet due to lower image resolutions and because image processing does not remove all atmospheric interference of the signal.

LAI has a strong relationship with the deciduousness in this forest typology. The increase of LAI indicates that the sprouting and growth of leaves increase until a maximum, synchronously with the reduction of deciduousness, when it reaches a minimum, and the reduction of leaf area starts, synchronously with the increase of the deciduousness. In this stage, the deciduousness drives the reduction of LAI, because in this period the leaf production practically stops.

Figs. 6-9 show graphical relationships between dry leaf and climate variables to sites 51, 61 and 81. Deciduousness phenomenon explains the expected relationships. The dry leaves have significant correlation with all variables, exception to maximum temperature (Fig. 6). The large correlations of dry leaves occurred with minimal temperature and hydric deficiency variables (Figs. 6 and 8) is the main cause of deciduousness.

On site 81, NDVI of images of Landsat 8 OLI was saturated a few times (Fig. 5), perhaps due to large values of green biomass. NDVI saturation in dense plant coverage affects the relation between LAI and NDVI, which occurs especially in ombrophilous typologies. The site 81 is classified as rain forest by IBGE, and is predominantly classified as Seasonal forest always green by Costa, T. C. C., et al. [24]. Another possible cause of NDVI saturation is amplitude changes of red and near infrared bands in Landsat 8. Roy, D. P., et al. [25] verified that, in Landsat 8, NDVI is in average 5% bigger than in Landsat 7.

2.5 Regression Model

The deciduousness relationship with each descriptor variable (LAI, NDVI, temperature, relative humidity, evapotranspiration, rain, water balance and wind speed) generated the better equation with polynomial model on Eq. (1), with $R^2 = 80.7\%$.

$$Dlw(g.m^{-2}.month^{-1}) = 26.0807 + 19.5211 \times LAI - 50.0720 \times NDVI - 4.2752 \times TMin + 0.3567 \times UR18 - 0.1356 \times DEF - 21.47 \times WinSp18 - 1.7907 \times LAI^2 + 77.6983 \times NDVI^2 - 0.0965 \times TMin^2 + 0.00388 \times UR18^2 + 0.000795 \times DEF^2 + 10.3549 \times WinSp18^2 \quad (1)$$

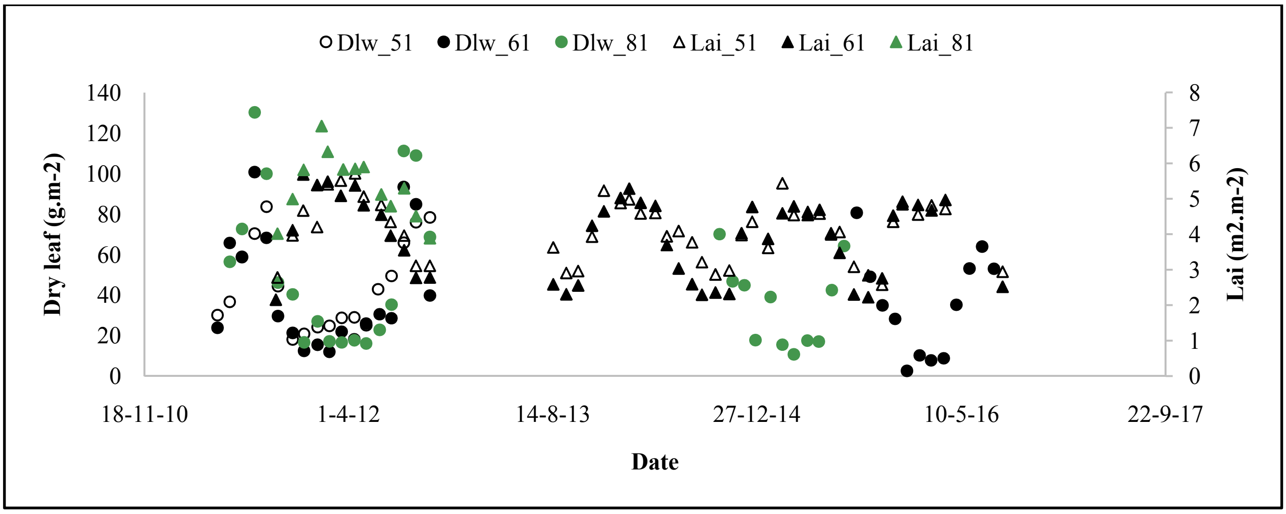

Fig. 4 Relation between dry leaf weight ($g \cdot m^{-2} \cdot period^{-1}$) and LAI ($m^2 \cdot m^{-2}$) in sites 51, 61 and 81.

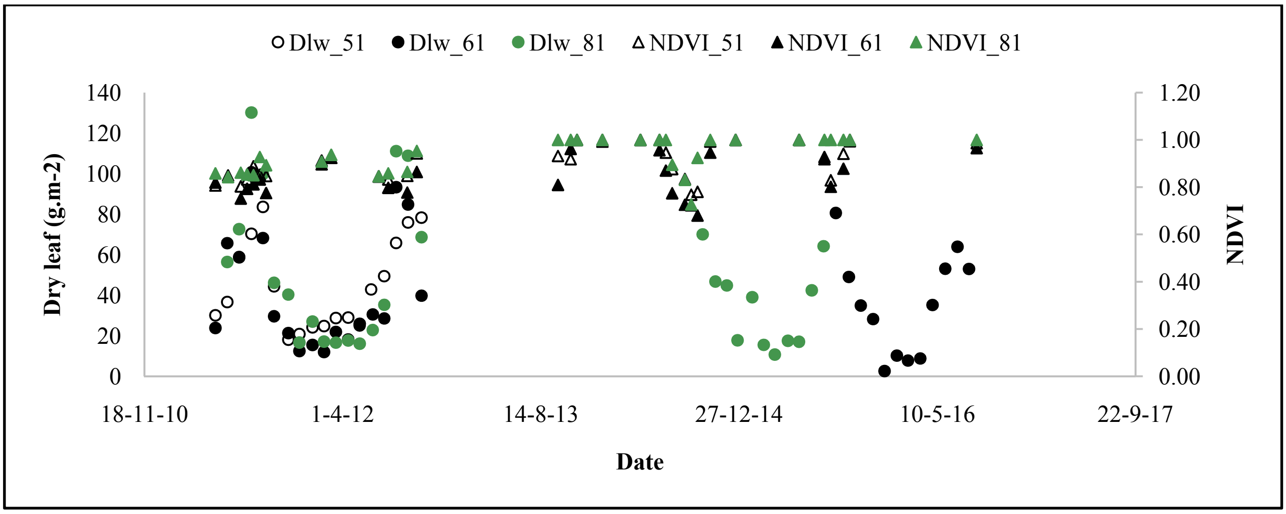

Fig. 5 Relations between dry leaf weight ($g \cdot m^{-2} \cdot period^{-1}$) and NDVI in sites 51, 61 and 81.

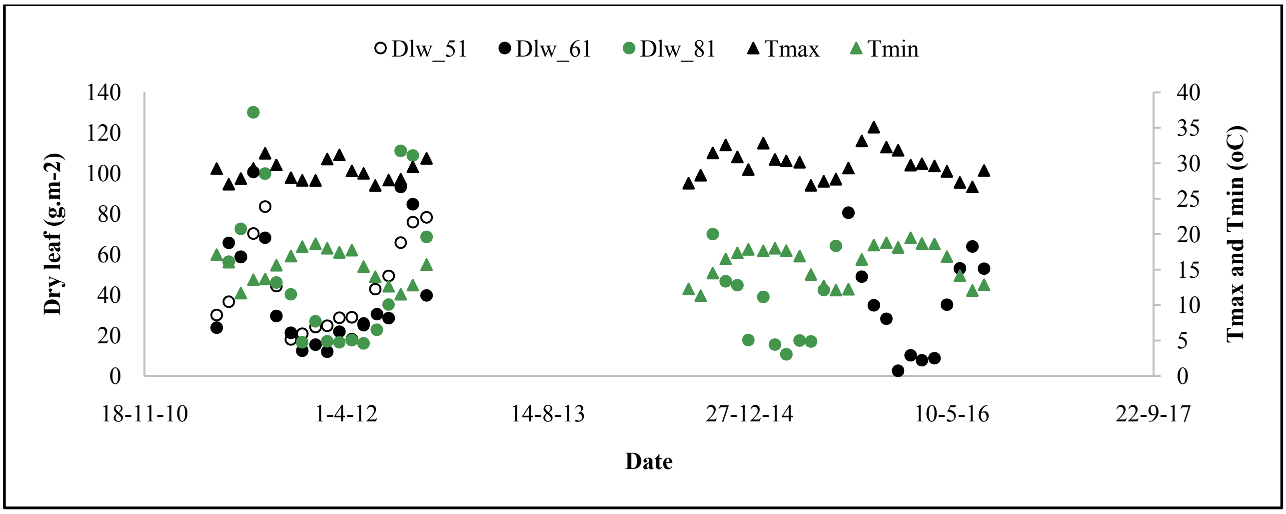

Fig. 6 Relations between dry leaf weight ($g \cdot m^{-2} \cdot period^{-1}$) and maximal and minimal temperature in sites 51, 61 and 81.

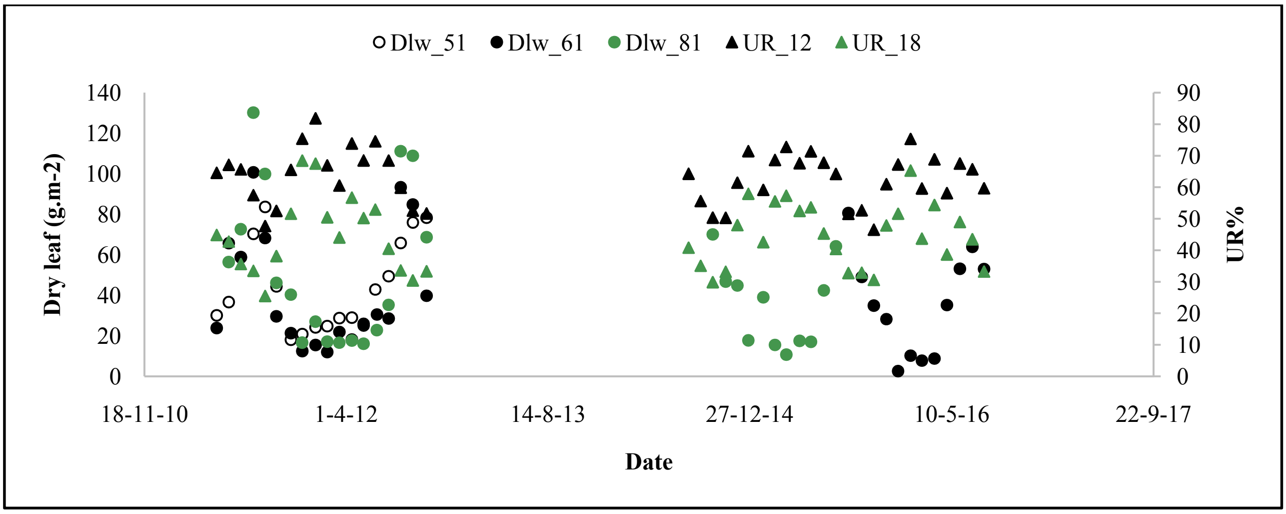

Fig. 7 Relations between dry leaf weight (g·m^{-2}·period^{-1}) and relative humidity on 12h and 18h UTC (Universal Coordinated Time) in sites 51, 61 and 81.

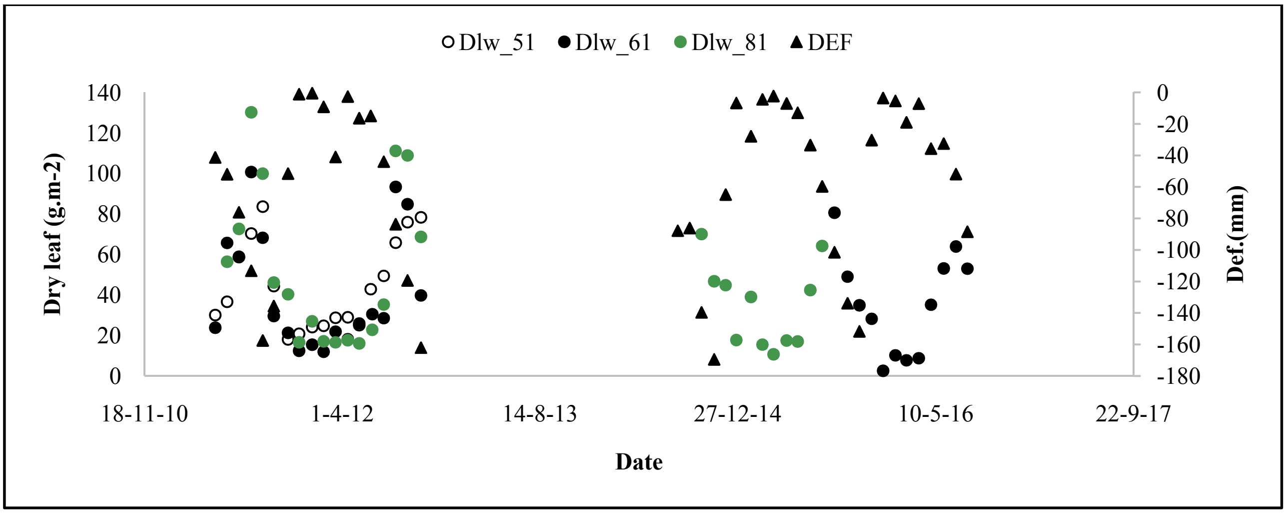

Fig. 8 Relations between dry leaf weight (g·m^{-2}·period^{-1}) and relative hydric deficit in sites 51, 61 and 81.

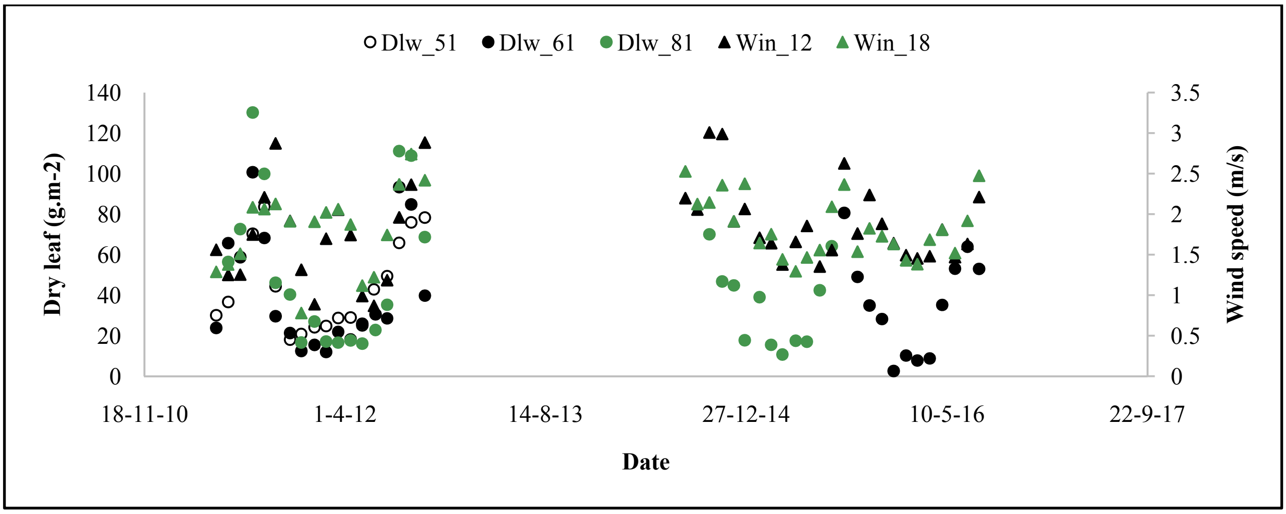

Fig. 9 Relations between dry leaf weight (g·m^{-2}·period^{-1}) and speed wind on 12h and 18h in sites 51, 61 and 81.

Figs. 10 (a) and (b) show the scatterplots. In Fig. 10 (a), the data present dispersion without bias along the 45º line. The integration of the monthly estimate in the 12-month period improves the precision. In Fig. 10 (b), the residuals did not present tendency with the observed variable value increase, indicating that there is not a serial correlation, and that heterogeneity of the variances was reduced. It was also verified that the inserted variables are enough to predict the variable Dlw.

Figs. 11 and 12 show the adjustment using the periods 2014/15, 2015/16. The before equations underestimated the bigger values, and the equation published in Costa, T. C. C., et al. [13] had the smaller tendency considering all values. The importance of the new equation is a smaller tendency for bigger Dlw estimations, with greater control including more explanatory variables: the minimal temperature, relative humidity and wind speed.

2.6 CO_2 Fixation Assessment

The predictions of the CO_2 capture by the adjusted deciduousness dynamics equation, for a period of 12 months in 2011/12 and 2015/16, were compared to the measured data. An annual quantity of carbon is deposited in the soil due to the sprouting process and the seasonal leaf growth and the posterior deposition of this biomass by the deciduousness process. Thus, for each period of 12 months, including the sequence of rainy and water deficit seasons, a measurable amount of CO_2 is captured by this forest typology, adding biomass in the trunks, branches and roots, determined by the growth of the vegetation.

However, the greater result of this account is that this amount of CO_2 captured occurs each year with renew and deposition of leaves, a sink of carbon.

The estimation of annual leaf deposition was accurate, according to the total of the monthly data (Table 4), with only two biggest errors, 20.2 and 23.1% in plot 611 of site 61, and 811 of site 81, respectively. The average fixation of CO_2 among the sites was 6.67 $Mg \cdot ha^{-1} \cdot yr^{-1}$ (observed values) and 6.37 $Mg \cdot ha^{-1} \cdot yr^{-1}$ (estimated values).

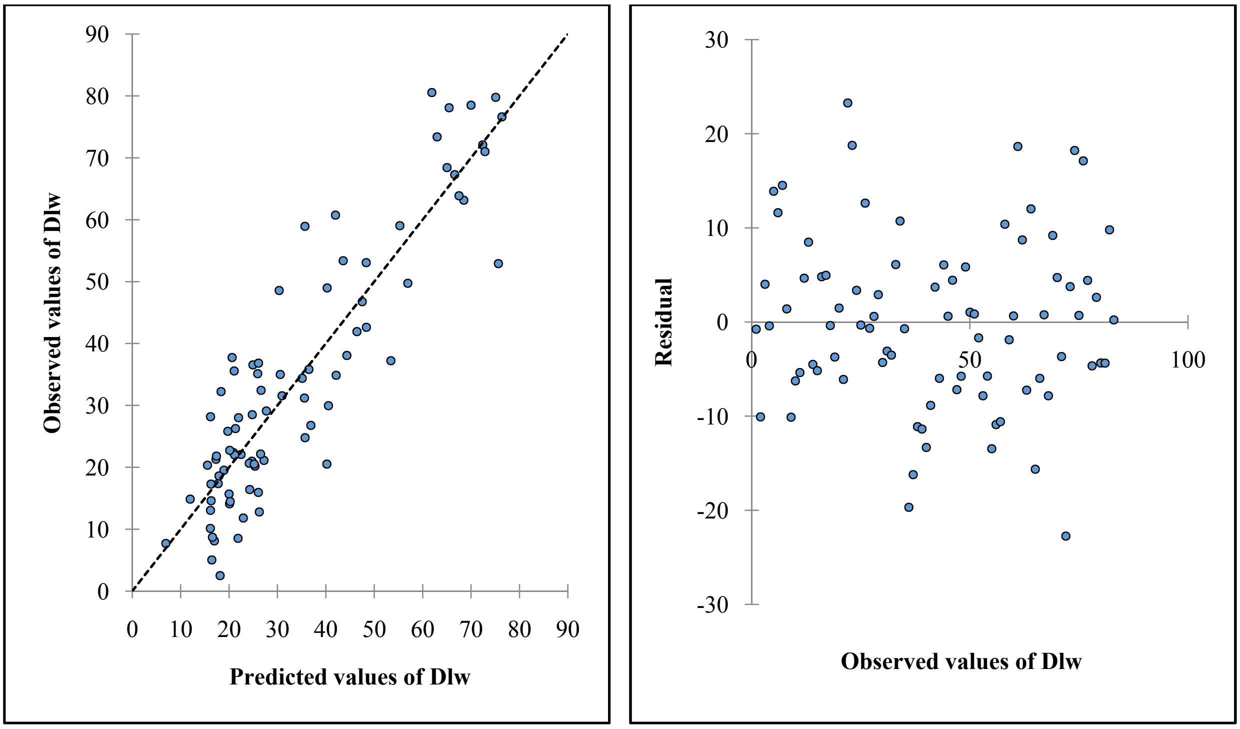

Fig. 10 (a) Observed data in function of the predicted data for the adjusted equation; (b) Dispersion of residuals in function of observed data.

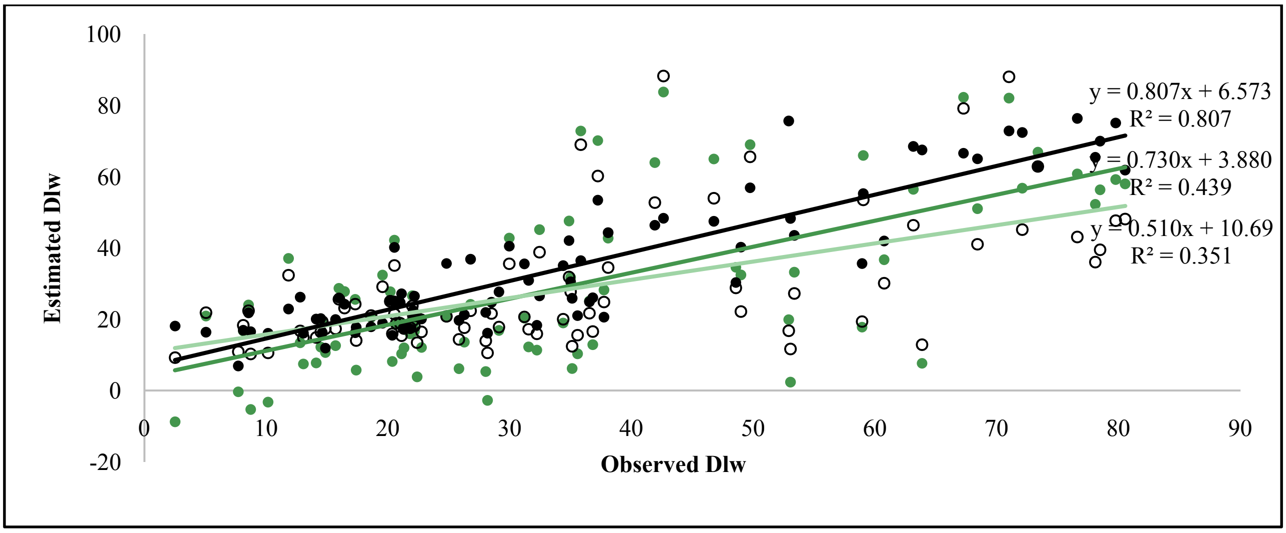

Fig. 11 Scatterplot of the Dlw observed and estimated by equation in [13] (●), by equation in [14] (○) and by equation (1) in this work (●).

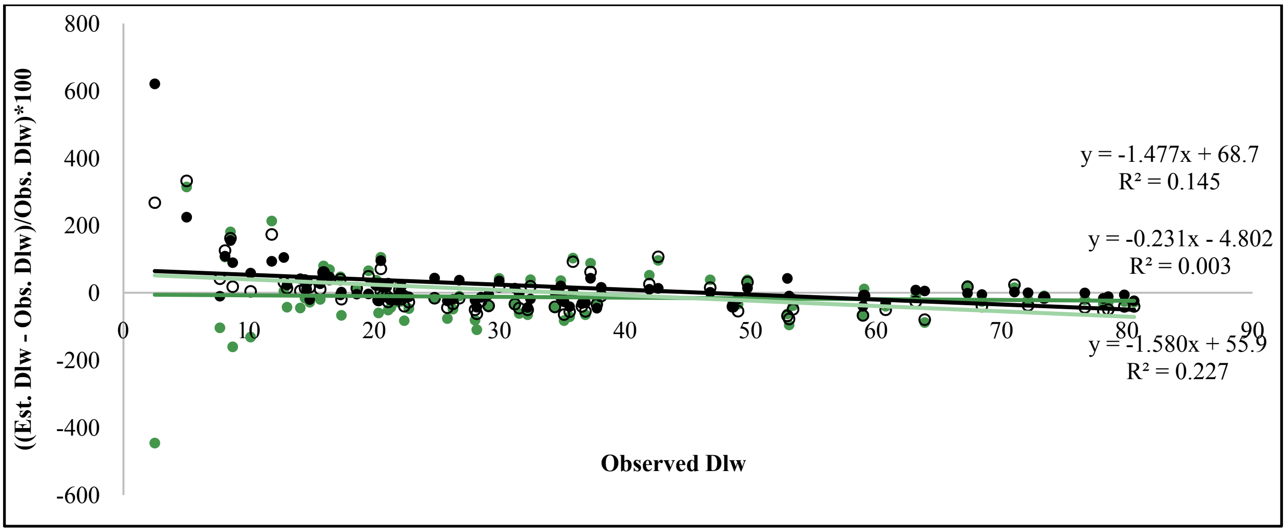

Fig. 12 Scatterplot of the observed Error (%) by equation in [13] (●), by equation in [14] (○) and (1) in this work (●).

Table 4 Observated, estimated data of Dlw and Error of estimation (%) to three equations; and observated and estimated data to fixed carbon in the leaves (C)* and captured CO_2 calculated by new equation.**

		Dlw	Eq.(2013)	Eq.(2014)	Eq.(new)	Er.(2013)	Er.(2014)	Er.(new)	C	C est.	CO_2	CO_2 est.
Period	Plot		($g \cdot m^{-2} \cdot yr^{-1}$)				(%)		($g \cdot m^{-2} \cdot yr^{-1}$)		($Mg \cdot ha^{-1} \cdot yr^{-1}$)	
11/10/11-13/09/12	511	447.4	371.0	338.9	430.3	-17.1	-24.3	-3.8	189.3	182.0	6.9	6.7
11/10/11-13/09/12	512	450.9	315.3	309.1	414.4	-30.1	-31.4	-8.1	190.7	175.3	7.0	6.4
11/10/11-13/09/12	611	467.4	372.7	383.9	372.9	-20.3	-17.9	-20.2	197.7	157.7	7.2	5.8
11/10/11-13/09/12	612	340.6	374.6	368.4	345.6	10.0	8.2	1.5	144.1	146.2	5.3	5.4
11/10/11-13/09/12	613	371.9	466.6	458.4	411.6	25.5	23.2	10.7	157.3	174.1	5.8	6.4
28/08/15-29/07/16	613	426.7	154.3	207.8	435.7	-63.8	-51.3	2.1	180.5	184.3	6.6	6.8
11/10/11-13/09/12	811	578.8	386.8	341.7	445.3	-33.2	-41.0	-23.1	244.8	188.4	9.0	6.9
27/08/14-28/07/15	811	549.5	-	-	-							

* considering 42.3% of the biomass (average value of contents in leaves of forest species obtained by Watzlawick, L. F., et al. [26].

** by the equivalence of atomic weight between C (12 g) and CO_2 (44 g).

4. Conclusions

It can confirm the relationship of climatic variables and biophysics remote sensing variables with deciduousness phenomenon in semideciduous seasonal forest. The new model proposed is nonlinear and included more variables to improve consistence. This research needs other experiments to new interannual validations and models test. These sites of the deciduous seasonal tropical forest were confirmed as able to capture average 6.5 tons of CO_2 per hectare/year, only due to the deciduousness phenomenon, which will depend on the regeneration stage and forest conservation, besides the other factors used in this equation.

Acknowledgements

This study is the last result of project CNPq561864/2010-1 "Parameters of forest fragmentation as subsidy for the environment quality and recovery of degraded environments". The author would like to thank the intern team who participated in the acquisition of the data in the second phase of this work: Francimar Roberto da Silva, Vilmar Martins, Leon Sulfierry and Letícia Almeida. The author also would like to thank Antonio Claudio da Silva Barros for the proofreading.

References

[1] Konig, F. G., Schumacher, M. V., Brun, E. J., and Seling, I. 2002. "Evaluation of the Seasonal Variation of Litter Production in a Seasonal Deciduous Forest in Santa Maria, RS." *Revista Árvore* 26 (4): 429-35.

[2] Brun, E. J., Schumacher, M. V., and Vaccaro, S. 1999. "Produção de serapilheira e devolução denutrientes em três fases sucessionais de uma Floresta Estacional Decidual no município deSanta Tereza (RS)." In *Anais do Simpósio de Fertilização e Nutrição Florestal, Piracicaba*. Piracicaba: ESALQ, 348-64. (in Portuguese)

[3] Feger, K. H., and Raspe, S. 1998. "Ecosystem Research in the Black Forest: Effects of Atmospheric Inputs and Restabilization Measures on the Water and Substance Balance of Spruce Forests." In *Verbundprojekt ARINUS, Reihe Umweltforschung in Baden-Württemberg.* Landsberg: Ecomed-Verlag, 1-18.

[4] Cunha, G. C. 1997. *Aspectos da Ciclagem de Nutrientes em Diferentes Fases Sucessionais de uma Floresta Estacional do Rio Grande do Sul*, (Dissertation) Piracicaba: Escola Superior de Agricultura "Luiz de Queiroz", 86. (in Portuguese)

[5] Soudani, K., Hmimina, G., Delpierre, N., Pontailler, J.-Y., Aubinet, M., Bonal, D., et al. 2012. "Ground-based Network of NDVI Measurements for Tracking Temporal Dynamics of Canopy Structure and Vegetation Phenology in Different Biomes." *Remote Sensing of Environment* 123: 234-45.

[6] Moreira, F. M. S., and Siqueira, J. O. 2002. *Microbiologia e bioquímica do solo*. Lavras: UFLA, 625. (in Portuguese)

[7] Barichello, L. R., Schumacher, M. V., Vogel, H. L. M., and Dallago, J. S. 2000. "Quantificação dos Nutrientes no Solo e Serapilheira de Diferentes Estágios Sucessionais em um Sistema de Agricultura Migratória." In *Resumos expandidos da Reunião Sul Brasileira de Ciência do Solo*. Pelotas (CD-ROM). (in Portuguese)

[8] Potithep, S., Nagai, S., Nasahara, K. N., Moraoka, H., and Suzuki, R. 2013. "Two Separate Periods of the LAI-Vis Relationships Using in situ Measurements in a Deciduous Broadleaf Forest." *Agricultural and Forest Meteorology* 169: 148-55.

[9] Kale, M., Singh, S., and Roy, P. S. 2005. "Estimation of Leaf Area Index in Dry Deciduous Forests from IRS-WiFS in Central India. Technical Note." *International Journal of Remote Sensing* 26 (21): 4855-67.

[10] Zhang, X., Friedl, M. A., Schaaf, C. B., and Strahler, A. H. 2004. "Climate Controls on Vegetation Phonological Patterns in Northern Mid- and High Latitudes Inferred from MODIS Data." *Global Change Biology* 10: 1133-45.

[11] Zhang, X., Friedl, M. A., Schaaf, C. B., Strahler, A. H., Hodges, J. C. F., Gao, F. et al. 2003. "Monitoring Vegetation Phenology Using MODIS." *Remote Sensing of Environment* 84: 471-5.

[12] Fensholt, R., Inge Sandholt, I., and Rasmussen, M. S. 2004. "Evaluation of MODIS LAI, fAPAR and the Relation between fAPAR and NDVI in a Semi-arid Environment Using in situ Measurements." *Remote Sensing of Environment* 91: 490-507.

[13] Costa, T. C. C., Ribeiro, J. L., Ferreira, F. N., Raid, M. A. M., and Miranda, G. A. 2013 Relações entre caducifolia e reenfolhamento da Floresta Estacional Semidecidual com Lai e ndvi. Anais XVI Simpósio Brasileiro de Sensoriamento Remoto-SBSR, Foz do Iguaçu, PR, Brasil, INPE, 3443-3450. (in Portuguese)

[14] Costa, T. C. C., Viana, J. H. M., and Ribeiro, J. L. 2014 "Semideciduous Seasonal Forest Production of Leaves

and Deciduousness in Function of the Water Balance, LAI, and NDVI." *International Journal of Ecology*. 2014: 15.

[15] Peel, M. C., Finlayson, B. L., and McMahon, T. A. 2007. "Updated World Map of the Koppen—Geiger Climate Classification." *Hydrology and Earth System Sciences* 11 (5): 1633-44.

[16] Gomide, R. L., Albuquerque, P. E. P., Andrade, C. L. T., Duraes, F. O. M., and Viana, J. H. M. 2006. "Climatic Characterization and Determination of the Water Requirements of Crops of the Precision Specific Site in Sete Lagoas for Phenotyping of Cereal Genotypes Tolerant to Drought." Alice Repository. Accessed October 30, 2014. http://www.alice.cnptia.embrapa.br/handle/doc/490096.

[17] USDA. 1999. "Soil Taxonomy: A Basic System of Soil Classification for Making and Interpreting Soil Surveys." *Agriculture Handbook* 436: 871.

[18] Li-Cor. 2011. *LAI-2200 Plant Canopy Analyzer: Instruction Manual.* Lincoln: Li-Cor Biosciences.

[19] Eastman, J. R. 2009. "ATMOSC", IDRISI Help System. Accessed in IDRISI Taiga. Worcester, MA: Clark University.

[20] Chavez, P. S. J. 1988. "An Improved Dark-object Subtraction Technique for Atmospheric Scattering Correction of Multispectral Data." *Remote Sensing of Environment* 24 (3): 459-79.

[21] Gürtler, S., Epiphanio, J. C. N., Luiz, A. J. B., and Formaggio, A. R. 2005. "Electronic Spreadsheet to Acquire the Reflectance from the TM and ETM+Landsat Images." *Revista Brasileira de Cartografia* 57 (2): 162-7.

[22] Bird, R. E., and Riordan, C. 1986. "Simple Solar Spectral Model for Direct and Diffuse Irradiance on Horizontal and Tilted Planes at the Earth's Surface for Cloudless Atmospheres." *Journal of Climate and Applied Meteorology* 25: 87-97.

[23] Maghrabi, A., and Al Dajani, H. M. 2013. "Estimation of Precipitable Water Vapour Using Vapour Pressure and Air Temperature in an Arid Region in Central Saudi Arabia." *Journal of the Association of Arab Universities for Basic and Applied Sciences* 14: 1-8.

[24] Costa, T. C. C., Silva, A. F., Temponi, L. M., and Viana, J. H. M. 2015. "Probabilistic Classification of Tree and Shrub Vegetation on Phytogeographic System." *Journal of Environmental Science and Engineering B* 4 (2015): 315-30. doi:10.17265/2162-5263/2015.06.003.

[25] Roy D. P., Kovalskyy, V., Zhang, H. K., Vermote, E. F., Yan, L., Kumar S. S., et al. "Characterization of Landsat-7 to Landsat-8 Reflective Wavelength and Normalized Difference Vegetation Index Continuity." *Remote Sensing of Environment* 185 (2016) 57-70.

[26] Watzlawick, L. F., Ebling, A. A., Rodrigues, A. L., Veres, Q. J. I., and Lima, A. M. 2011. "Organic Carbon Levels Variation in Tree Species of the MIXED Rain Forest." *Floresta e Ambiente* 18 (3): 248-58.